FISSION DYNAMICS WITH MICROSCOPIC LEVEL DENSITIES*

D. Ward[a], B.G. Carlsson[a], Th. Døssing[b], P. Möller[c]
J. Randrup[d], S. Åberg[a]

[a]Mathematical Physics, Lund University, 221 00 Lund, Sweden
[b]Niels Bohr Institute, Copenhagen University, 2100 Copenhagen, Denmark
[c]Los Alamos National Laboratory, Los Alamos, New Mexico 87545, USA
[d]Lawrence Berkeley National Laboratory, Berkeley, California 94720, USA

(Received January 23, 2017)

We present a consistent framework for treating the energy and angular-momentum dependence of the shape evolution in the nuclear fission. It combines microscopically calculated level densities with the Metropolis-walk method, has no new parameters, and can elucidate the energy-dependent influence of pairing and shell effects on the dynamics of warm nuclei.

DOI:10.5506/APhysPolBSupp.10.201

1. Introduction

Soon after the discovery of nuclear fission in 1938 [1], it was recognized that the process can be viewed qualitatively as an evolution of the nuclear shape from that of a single compound nucleus to two receding fragments [2,3] and that Langevin transport theory provides an appropriate model framework [3, 4]. A number of Langevin treatments of fission have been successfully developed and applied for excitations high enough to render the dynamics macroscopic, see, for example, Refs. [5–7].

If the collective shape dynamics is idealized as being highly dissipative, then the Langevin equation reduces to the Smoluchowski equation in which the evolution depends on the balance between the driving force provided by the potential energy of deformation and the dissipative force resulting from the coupling of the collective degrees of freedom to the remaining system. In this limit, it has proven possible to describe the Brownian shape motion as a Metropolis walk on the associated multi-dimensional deformation-energy

* Presented by J. Randrup at the XXIII Nuclear Physics Workshop "Marie and Pierre Curie", Kazimierz Dolny, Poland, September 27–October 2, 2016.

surface [8]. This calculationally simple method has yielded remarkably good results for the fission-fragment mass distributions [9] and it has made it possible to predict fission-fragment mass distributions for poorly explored regions of the nuclear chart [10,11].

2. Combinatorial level density

In Ref. [12], a method was developed for microscopic calculations of level densities for deformed nuclei and it has been adapted to the fission process [13]. For a specified shape $\boldsymbol{\chi}$, the single-particle levels for protons and neutrons needed for the combinatorial calculation of the level density are obtained by solving the Schrödinger equation in the associated folded-Yukawa potential. These are the same levels as those previously used in Ref. [14] to calculate the microscopic shell and pairing energies in the construction of the deformation energy surface, thus guaranteeing consistency of the approach. The corresponding local many-body vacuum state $|0;\boldsymbol{\chi}\rangle$ has N neutrons and Z protons filling the lowest single-particle states, and the uncorrelated excited states consist of all multiple particle–hole excitations

$$|i;\boldsymbol{\chi}\rangle \;=\; \prod_{n\geq 1} a^{\dagger}_{\nu_n^{(i)}} a_{\mu_n^{(i)}} |0;\boldsymbol{\chi}\rangle\,. \tag{1}$$

For each many-body state $|i;\boldsymbol{\chi}\rangle$, blocked BCS calculations for neutrons and protons separately provide the state-dependent pairing gaps, $\Delta_i^n(\boldsymbol{\chi})$ and $\Delta_i^p(\boldsymbol{\chi})$, respectively, and the energy of the correlated intrinsic many-body state, $E_i(\boldsymbol{\chi}) = E_i^n(\boldsymbol{\chi}) + E_i^p(\boldsymbol{\chi})$.

For each such an intrinsic state, the angular momentum along the nuclear symmetry axis is denoted by K_i and it is assumed that it forms a rotational band head. The resulting total angular momenta I may then take on the values $I = K_i, (K_i+1), (K_i+2), \ldots$ and the corresponding rotational energies of the band members are

$$E_i^{\mathrm{rot}}(I;\boldsymbol{\chi}) \;=\; \frac{I(I+1) - K_i(\boldsymbol{\chi})^2}{2\mathcal{J}_{\perp}\left(\boldsymbol{\chi}, \Delta_i^n(\boldsymbol{\chi}), \Delta_i^p(\boldsymbol{\chi})\right)}\,. \tag{2}$$

The moment of inertia $\mathcal{J}_{\perp}$ is approximated by the moment of inertia of a rigid body with the shape $\boldsymbol{\chi}$, modified by the calculated pairing gaps for the state [15].

In Ref. [12], it was found that the enhancements arising from collective vibrational modes are unimportant and they are, therefore, ignored in the present fission applications. The total energy of a state is then given by

$$E_i(I,\boldsymbol{\chi}) \;=\; E_i^n(\boldsymbol{\chi}) + E_i^p(\boldsymbol{\chi}) + E_i^{\mathrm{rot}}(I;\boldsymbol{\chi})\,. \tag{3}$$

For each shape $\boldsymbol{\chi}$, the resulting states are binned according to their energy E_i and their total angular momentum I; the bin width was taken as $\Delta E = 200$ keV. The sensitivity of our results to the bin size has been tested and it was found that a doubling or tripling of ΔE produces negligible changes in the calculated mass distributions.

3. Shape evolution

The description of nuclear fission as a generalized Brownian motion builds on the assumption that the evolving nucleus can be characterized by its shape degrees of freedom $\boldsymbol{\chi}$. The associated shape parameters are treated as classical variables that are coupled dissipatively to the remaining microscopic degrees of freedom. The resulting large-amplitude collective motion then exhibits a strongly damped diffusive evolution that can be described as a random walk on the associated multi-dimensional potential-energy surface $U(\boldsymbol{\chi})$. When the values of the potential are available on a (five-dimensional) lattice of shapes [14], the Smoluchowski equation can be approximately simulated by means of a random walk on this lattice [8].

Because the random walk must satisfy detailed balance, the following relation must hold between the rates of transition between one lattice site $\boldsymbol{\chi}$ and another $\boldsymbol{\chi}'$, and the corresponding statistical weights

$$\nu\left(\boldsymbol{\chi} \to \boldsymbol{\chi}'\right) / \nu\left(\boldsymbol{\chi}' \to \boldsymbol{\chi}\right) \;=\; \rho\left(\boldsymbol{\chi}'\right) / \rho(\boldsymbol{\chi})\,, \tag{4}$$

where $\rho(\boldsymbol{\chi})$ is the level density at the lattice site having the shape $\boldsymbol{\chi}$. This condition can be satisfied in many ways and the Metropolis procedure [16] is merely one particularly simple realization: A proposed shape change from $\boldsymbol{\chi}$ to $\boldsymbol{\chi}'$ is accepted unconditionally if $\rho(\boldsymbol{\chi}') > \rho(\boldsymbol{\chi})$, whereas it is accepted only with the probability $\rho(\boldsymbol{\chi}')/\rho(\boldsymbol{\chi})$ otherwise; it is readily verified that this procedure satisfies a detailed balance.

In Ref. [8] and all subsequent applications until recently [13], smooth Fermi-gas level-density expressions were used. The ratio between the level densities for neighboring lattice sites could, therefore, be approximated as

$$\rho\left(\boldsymbol{\chi}'\right) / \rho(\boldsymbol{\chi}) \;\approx\; \exp(-\Delta U/T)\,, \tag{5}$$

where $\Delta U = U(\boldsymbol{\chi}') - U(\boldsymbol{\chi})$ is the change in the potential energy associated with the proposed shape change and $T = 1/[\partial \ln \rho(E^*)/\partial E^*]$ is the local nuclear temperature. In the new development [13], we wish to account for pairing correlations and shell effects and we, therefore, use the microscopic level densities (see Sect. 2) to evaluate the required ratios $\rho(\boldsymbol{\chi}')/\rho(\boldsymbol{\chi})$.

The Metropolis walks were performed on a discrete lattice of more than five million shapes given in the three-quadratic-surface parametrization [17]. The five independent parameters characterizing a shape are the overall elon-

gation of the nucleus (in terms of the reduced quadrupole moment q_2), the constriction of the central part (in terms of the neck radius c), the spheroidal deformations $\varepsilon_{\rm f1}$ and $\varepsilon_{\rm f2}$ of the two nascent fragments, and the reflection (mass) asymmetry $\alpha_{\rm g}$.

4. Analytical extrapolation

Because the computational effort required by the combinatorial method grows exponentially with excitation, it is practically important to develop a simple way of extending the results to high energy. We do that by switching to an analytical expression at $E^*(\boldsymbol{\chi}) \approx 6$ MeV, below which most of the specific structure effects, such as spectral gaps or non-monotonic behavior, have washed out. In this way, important structures in the level density are maintained, while the numerical calculations are kept to a manageable level (about 3 CPU seconds per shape). For each particular shape $\boldsymbol{\chi}$, the extrapolation makes use of its specific shell and pairing energies, $E_{\rm sh}(\boldsymbol{\chi})$ and $E_{\rm pc}(\boldsymbol{\chi})$. Their influence diminishes with increasing energy and the level density approaches the analytical expression for a Fermi gas.

We employ the following simple analytical Fermi-gas expression [18], which is suitable for deformed nuclei with a fixed small angular momentum

$$\rho\,(N, Z, E^*(\boldsymbol{\chi}), I) = \; C(\boldsymbol{\chi})\, E_{\rm intr}^{-3/2} \exp\left(2\sqrt{a_0 E}\right)\,, \tag{6}$$

where $E_{\rm intr} = E^*(\boldsymbol{\chi}) - I(I+1)\hbar^2/2\mathcal{J}_\perp(\boldsymbol{\chi})$ is the approximate intrinsic energy. The single-particle level-density parameter is $a_0 = A/e_0$ for a nucleus having mass number A and the constant e_0 is determined below.

Accounting for the different energy scales of shell effects and pairing effects, we introduce a backshifted intrinsic excitation energy $\tilde{E}_{\rm intr}$, which is similar to the effective excitation $E^*_{\rm eff}$ of Ref. [9] and can be considered a generalization of the prescription originally employed by Ignatyuk *et al.* [19]

$$\begin{aligned}\tilde{E}_{\rm intr}(\boldsymbol{\chi}) \;&=\; E_{\rm intr}(\boldsymbol{\chi}) \;+\; \left(1 - e^{-E_{\rm intr}(\boldsymbol{\chi})/E_{\rm d,sh}}\right) E_{\rm sh} \\ &\quad+\; \left(1 - e^{-E_{\rm intr}(\boldsymbol{\chi})/E_{\rm d,pc}}\right) E_{\rm pc}\,.\end{aligned} \tag{7}$$

Here, $E_{\rm sh}(\boldsymbol{\chi})$ is the shell-correction energy and $E_{\rm pc}(\boldsymbol{\chi})$ is the pairing condensation energy, both calculated for the lowest state at the given shape $\boldsymbol{\chi}$. The full backshifted energy, $\tilde{E}_{\rm intr} = E_{\rm intr} + E_{\rm sh} + E_{\rm pc}$, emerges when $E_{\rm intr}$ is much larger than both damping scales.

The damping parameter $E_{\rm d,sh}$ sets the energy scale for the melting of shell structure and the damping parameter $E_{\rm d,pc}$ is the corresponding energy scale for the melting of pairing correlations. For simplicity, both quantities are here assumed to be common to all shapes. By fitting the analytic expression

for a number of typical shapes, optimal values of $E_{\mathrm{d,sh}}$, $E_{\mathrm{d,pc}}$, and e_0 are determined and they are then applied for all shapes. The normalization constant $C(\boldsymbol{\chi})$ in (6) is determined by continuity with the corresponding microscopic value at the matching energy.

The validity of the analytical extrapolation is illustrated in Fig. 1.

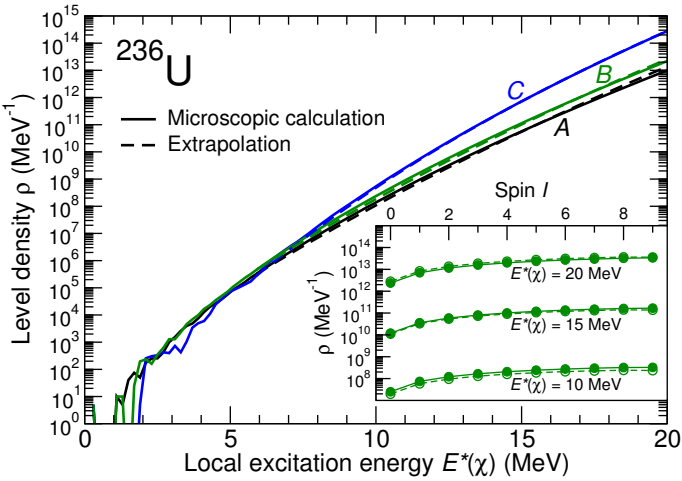

Fig. 1. Microscopic level densities (solid lines) compared to extrapolated values (dashed lines). Three different deformations for ^{236}U are considered: the second minimum (A), the asymmetric second saddle (B), and an elongated symmetric shape close to the outer barrier (C). Extrapolated values are shown for local excitation energies $E^*(\boldsymbol{\chi}) \geq 6$ MeV. The inset shows the angular momentum dependence of the level density at the asymmetric saddle (B) for different excitation energies.

5. Energy dependence of the fragment yield

The use of microscopic level densities is particularly well-suited for studying the dependence of the shape evolution on the total excitation energy of the fissioning system because the microscopic pairing and shell effects automatically wash out as the energy is raised. This is illustrated in Fig. 2.

The preliminary treatment in Ref. [9] used an energy-dependent effective potential obtained by suppressing the microscopic term with a factor of the form $\mathcal{S}(E^*) = (1+c)/[\exp(E^*/E_{\mathrm{damp}})+c]$, which decreases from one to zero as the excitation E^* is raised

$$U_E(\boldsymbol{\chi}) \;=\; U_{\mathrm{macro}}(\boldsymbol{\chi}) \;+\; \mathcal{S}(E^*(\boldsymbol{\chi}))\, E_{\mathrm{micro}}(\boldsymbol{\chi})\,. \tag{8}$$

The local statistical weights were then obtained by means of a simplified Fermi-gas level density, $\rho_{\mathrm{eff}}(\boldsymbol{\chi}) = \rho_{\mathrm{FG}}(E_{\mathrm{total}} - U_E(\boldsymbol{\chi}))$.

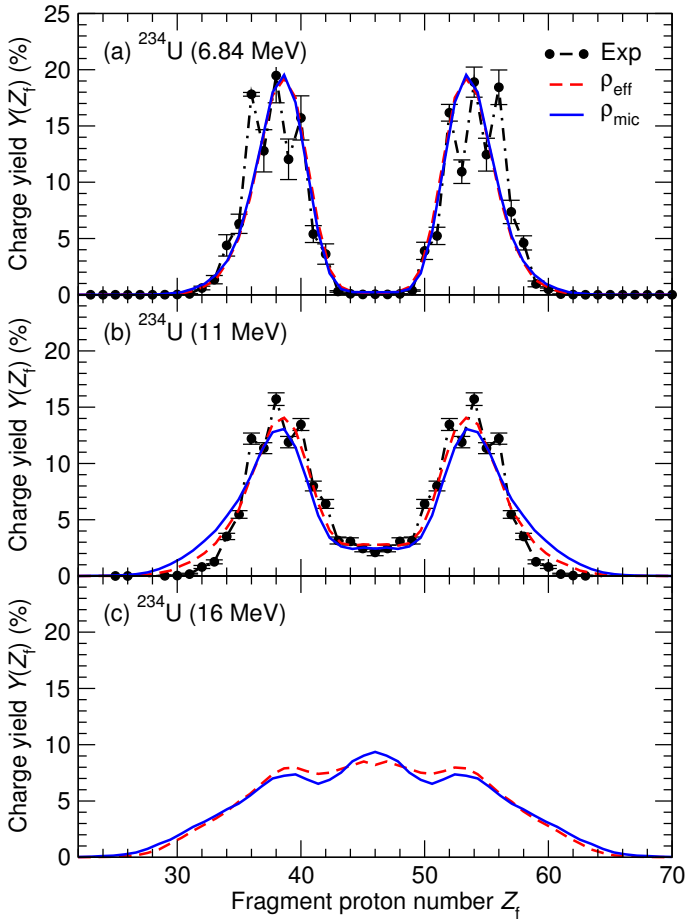

Fig. 2. (Color online) Fission-fragment charge distributions for ^{234}U at three different excitation energies E^* [MeV]: 6.84 (a), 11 (b), and 16 (c). The solid/blue curves have been obtained with the microscopic level densities, while the dashed/red curves were calculated with the effective level density $\rho_{\rm eff}$ introduced in Ref. [9]. The results for $E^* = 6.84$ MeV are compared to $(n_{\rm th}, f)$ data [20], while those for $E^* = 11$ MeV are compared to (γ, f) data [21]. The calculated results for $E^* = 6.84$ MeV are practically identical and both are in a good agreement with the experimental data. For $E^* = 11$ MeV, the current approach reproduces the symmetric yield of around 2%, while the very asymmetric yields are too large. The calculated yields for $E^* = 16$ MeV are also quite similar.

5.1. The symmetric yield

The importance of taking account of nuclear structure effects in the level density is well illustrated by the energy dependence of the fission-fragment yield for symmetric splits, see Fig. 3. The standard calculation leads to a local maximum at $E^* = 7$ MeV, followed by a local minimum at 8 MeV; this bump is followed by a second bump ending with an inflection at around 10 MeV. The experimental data exhibit a qualitatively similar behavior, in particular a local maximum at $E^* = 7$ MeV. Without pairing, the absence of a gap produces a larger level density, especially for shapes with positive shell corrections, where both the gap and the single-particle level density are larger. Thus the symmetric yield is highly sensitive to the pairing properties of the level density.

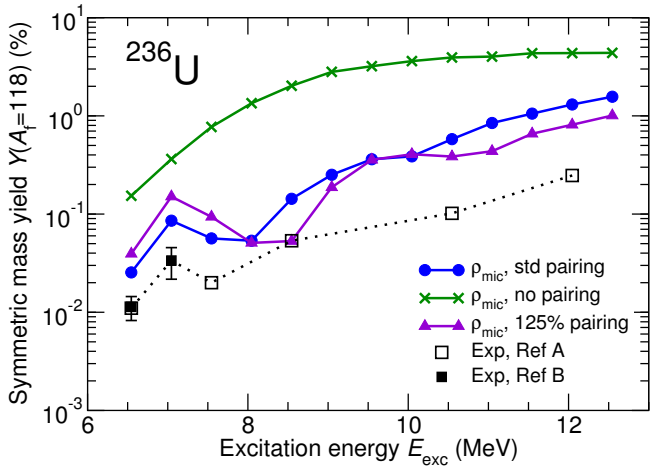

Fig. 3. (Color online) The dependence of the symmetric mass yield for ^{236}U on the excitation energy. In addition to the standard calculation (blue circles) two additional calculations are shown — one where the level densities are obtained without pairing (green crosses) and one where the pairing strength is increased by 25% (triangles). (The potential-energy surface used in the three calculations is the same, consistent with standard pairing.) Also shown are experimental data from Ref. [22] (open squares) and Ref. [20] (filled squares).

6. Concluding remarks

We have refined the Metropolis-walk approximation to the Brownian-motion treatment of fission dynamics [8] by employing microscopic local level densities obtained by a recently developed combinatorial method [12]. Because the single-particle levels used are the same as those employed for

the macroscopic–microscopic calculation of the potential-energy surfaces, the approach is consistent and no new parameters need be introduced. Moreover, the combinatorial procedure provides access to the level density for a fixed value of angular momentum. We have obtained the local level density $\rho(N, Z, E, I; \boldsymbol{\chi})$ for over 5 million shapes of several nuclei in the uranium region and for angular momenta up to $I = 9$.

We calculated fission fragment charge distributions for ^{226}Th, ^{234,236}U, and ^{240}Pu using these parameter-free microscopic level densities with the Metropolis-walk method. The agreement with experimental data was on par with or better than the yields obtained previously with a phenomenological level-density parametrization [9]. The angular-momentum dependence of the fission yields was found to be relatively small and decreasing with increasing excitation energy.

Because the microscopic level densities automatically contain the diminishing effects of pairing correlations and shell structure, the present refined model makes it possible to make more detailed predictions for the energy dependence of the fission yields. The gradual transition from asymmetric to symmetric fission and the detailed energy dependence of the symmetric yield were studied.

Particularly interesting is the finding that the symmetric fragment yield is not monotonically increasing with excitation energy. This perhaps counterintuitive effect appears to be a result of the large pairing correlations for shapes with positive shell-correction energies separating the asymmetric-fission path from symmetric shapes. It is in this connection intriguing that a recent experiment has reported a non-monotonic energy dependence of the asymmetric peak shape in the fragment mass yields for fission of ^{240}Pu [23]. We plan to investigate these phenomena in more detail.

The present refined model provides a consistent and computationally manageable theoretical framework for studying large-scale collective motion of warm nuclear systems far from equilibrium and, in particular, it provides a unique tool for calculating energy-dependent fission fragment mass distributions. The present work extends the use of microscopic level densities from nuclei in shape equilibrium to arbitrary shapes and our present studies have revealed the intriguing possibility that the pairing interaction in shapes far from equilibrium may manifest itself in a measurable manner through the energy dependence of the fission yields.

We are grateful to N. Schunck, A. Tonchev, and R. Vogt for discussions, helpful comments, and valuable suggestions. This work was supported by the Swedish Natural Science Research Council (B.G.C. and S.Å.), by the National Nuclear Security Administration of the U.S. Department of Energy at Los Alamos National Laboratory under contract No. DE-AC52-06NA25396 (P.M.), and by the Office of Nuclear Physics in the U.S. Department of Energy's Office of Science under contract No. DE-AC02-05CH11231 (J.R.).

REFERENCES

[1] O. Hahn, F. Straßmann, *Naturwiss.* **27**, 11 (1939).
[2] L. Meitner, O.R. Frisch, *Nature* **143**, 239 (1939).
[3] N. Bohr, J.A. Wheeler, *Phys. Rev.* **56**, 426 (1939).
[4] H.A. Kramers, *Physica* **7**, 284 (1940).
[5] A.V. Karpov *et al.*, *Phys. Rev. C* **63**, 054610 (2001).
[6] P.N. Nadtochy *et al.*, *Phys. Rev. C* **65**, 064615 (2002).
[7] E.G. Ryabov *et al.*, *Phys. Rev. C* **78**, 044614 (2008).
[8] J. Randrup, P. Möller, *Phys. Rev. Lett.* **106**, 132503 (2011).
[9] J. Randrup, P. Möller, *Phys. Rev. C* **88**, 064606 (2013).
[10] P. Möller, J. Randrup, A.J. Sierk, *Phys. Rev. C* **85**, 024306 (2012).
[11] P. Möller, J. Randrup, *Phys. Rev. C* **91**, 044316 (2015).
[12] H. Uhrenholt *et al.*, *Nucl. Phys. A* **913**, 127 (2013).
[13] D. Ward *et al.*, *Phys. Rev. C* **95**, 024618 (2017).
[14] P. Möller, *Phys. Rev. C* **79**, 064304 (2009).
[15] R. Bengtsson, S. Åberg, *Phys. Lett. B* **172**, 277 (1986).
[16] N. Metropolis *et al.*, *J. Chem. Phys.* **21**, 1087 (1953).
[17] J.R. Nix, *Nucl. Phys. A* **130**, 241 (1969).
[18] T. Ericsson, *Adv. Phys.* **9**, 425 (1960).
[19] A.V. Ignatyuk, K.K. Istekov, G.N. Smirenkin, *Sov. J. Nucl. Phys.* **29**, 450 (1979).
[20] M.B. Chadwick *et al.*, *Nucl. Data Sheets* **112**, 2887 (2011).
[21] K.-H. Schmidt *et al.*, *Nucl. Phys. A* **665**, 221 (2000).
[22] L.E. Glendenin, J.E. Gindler, D.J. Henderson, J.W. Meadows, *Phys. Rev. C* **24**, 2600 (1981).
[23] M.E. Gooden *et al.*, *Nucl. Data Sheets* **131**, 319 (2016).